Title

Vessel wall MR imaging in Neuroradiology

Manuscript type

Review Articles

Abstract

Vessel wall MR imaging (VW-MRI) has been introduced into clinical practice and applied to a variety of diseases and its usefulness has been reported. High-resolution VW-MRI is essential in the diagnostic workup and provides more information than other routine MR imaging protocols. VW-MRI is useful in assessing lesion location, morphology, and severity. Additional information, such as vessel wall enhancement, which is useful in the differential diagnosis of atherosclerotic disease and vasculitis could be assessed by this special imaging technique. This review describes the VW-MRI technique and its clinical applications in arterial disease, venous disease, vasculitis, and leptomeningeal disease.

Key words

vessel wall MR imaging; 3D MRI; vessel wall enhancement; magnetization transfer; MR angiography; Delays Alternating with Nutation for Tailored Excitation

Abbreviations

Trial of Org 10 172 in Acute Stroke Treatment, TOAST;

vessel wall MR imaging, VW-MRI;

contrast enhanced, CE;

time-of-flight, TOF;

MR angiography, MRA;

CT angiography, CTA;

fast spin-echo, FSE;

variable flip angle refocusing pulse, VFA;

multiplanar reconstruction, MPR;

cerebrospinal fluid, CSF;

motion-sensitized driven equilibrium, MSDE;

Delays Alternating with Nutation for Tailored Excitation, DANTE;

magnetization transfer, MT;

signal to noise ratio, SNR;

intraplaque hemorrhage, IPH;

lipid-rich necrotic core, LRNC;

cervical artery dissection, CAD;

internal carotid artery dissection, ICAD;

vertebral artery dissection, VAD;

subarachnoid hemorrhage, SAH;

reversible cerebral vasoconstriction syndrome, RCVS;

middle cerebral artery, MCA;

convolutional neural network, CNN;

susceptibility-weighted imaging, SWI;

three-dimensional, 3D;

digital subtraction angiography, DSA;

primary angiitis of the central nervous system, PACNS;

giant cell arteritis, GCA;

fluorodeoxyglucose Positron emission tomography, FDG-PET;

arteritic anterior ischemic optic neuropathy, A-AION;

human immunodeficiency virus, HIV;

coronavirus disease 2019, COVID-19;

gradient echo, GRE;

Introduction

Ischemic stroke is the common neurologic diseases and following five broad subtypes has been classified to represent most clinical scenarios in the Trial of Org 10 172 in Acute Stroke Treatment (TOAST) system: large artery atherosclerosis, small artery occlusion, cardioembolism, other demonstrated cause, and undetermined cause [1,2]. Intracranial atherosclerosis is one of major causes of ischemic stroke, and vessel wall MR imaging (VW-MRI) is suitable for evaluation of intracranial atherosclerosis compared with other intraluminal imaging such as transcranial Doppler, time-of-flight (TOF) MR angiography (MRA), contrast enhanced (CE) CT angiography (CTA), and digital subtraction angiography (DSA). For these reasons, high-resolution VW-MRI has been gaining interest for detailed visualization of intracranial vessel walls. The subtype classification to determine the causes of stroke is important in clinical practices [1,2]. The evidence of extracranial or intracranial disease supports large artery atherosclerosis [3,4], and negative results on VW-MRI are also important for the subtype determination of cardioembolisms and undetermined causes.

VW-MRI has been introduced in clinical practices, applied to various diseases, and its usefulness has been reported. The purpose of this paper was to review imaging findings of VW-MRI.

Techniques of VW-MRI

VW-MRI has been used mainly to evaluate vulnerable plaque in extracranial carotid artery with 2D imaging such as double inversion recovery previously [5]. The drawbacks of 2D imaging are low slice-selective resolution compared with in-plane resolution, and partial volume effect. Technical development has provided various options for plaque imaging such as 3D fast spin-echo (FSE) imaging with variable flip angle refocusing pulse (VFA). Pseudo steady state can be achieved by prospectively controlled signal decay at the beginning of the echo train, thus constant signal intensity is maintained [6]. Black blood effect is brought about since phase dispersion arises from the intravoxel blood flow velocity variation as well as the uncompensated first-order gradient moment during each echo readout [7]. Further phase dispersion occurs due to stimulated echoes introduced by the low-flip-angle refocusing pulses [8,9].

3D MR imaging with high spatial resolution and improved anatomic coverage became possible by optimized and efficient k-space trajectories with sampling in both in-

plane and through-slab phase-encode directions [10]. Higher acceleration in phase and partition direction can be applied for 3D FSE with various techniques including compressed sensing [11,12], thus wide coverage and scan time reduction become possible. Availability of multiplanar reconstruction (MPR) for suitable visualization of vessel wall is another advantage of 3D imaging, and both vessel segment focused VW-MRI and whole brain VW-MRI have been performed recently [13].

VW-MRI techniques rely on blood flow to achieve blood-signal suppression. Incomplete signal suppression in the periphery of the lumen can mimic vessel wall thickening and/or wall enhancement. Recirculating or slow flow within an aneurysm, low velocity flow in a dilated artery, and retrograde filling of a branch artery via leptomeningeal collaterals may result in incomplete signal suppression [14,15]. Therefore, further intravoxel dephasing effect can be brought about by additional preparation pulses and followings have been developed to achieve better black blood effect as well as cerebrospinal fluid (CSF) suppression: Diffusion-sensitizing gradient preparation (motion-sensitized driven equilibrium, MSDE) [7,16], T2-prepared inversion recovery [17], a flip-down radiofrequency pulse module [18], and Delays Alternating with Nutation for Tailored Excitation (DANTE) [19,20]. Although many articles using VW-MRI with MSDE have been reported, DANTE has been reported to produce better signal

to noise ratio (SNR) compared with MSDE [20].

DANTE pulse is a continuous irradiation of short duration hard pulse with small flip angle, and it has been used for frequency selective excitation in NMR spectroscopy [21] and cardiac tagging [22]. Recently DANTE pulse is used for VW-MRI with the advantage of signal suppression of both blood flow and CSF signal [20,23-26]. CSF is known to affect vessel walls [27]. DANTE pulse is also used for intravascular signal suppression of arterial spin labeling [28], detection of brain metastasis [29], and neuromelanin-sensitive MRI due to certain magnetization transfer (MT) effect [30]. With acceleration of parallel imaging, high resolution vessel wall imaging using DANTE pulse can be available in clinically feasible scan time [30,31].

Deep learning application for VW-MRI

Deep learning technique have been introduced for acute ischemic stroke and plaque identification. Hyperdense middle cerebral artery (MCA) sign on CT is a well-known sign of acute embolism and nowadays deep learning-assisted identification has been introduced [32]. Moreover, convolutional neural network (CNN)-based domain adaptive lesion classification could locate target arteries and distinguish carotid atherosclerotic lesions [33].

Deep learning can be used for improvement of SNR, and CNN improved overall image quality for high resolution VW-MRI [34].

Clinical application of VW-MRI - Arterial diseases

Carotid artery plaque

Rupture of vulnerable plaque is known to be an important cause of stroke rather than the luminal stenosis [35]. Chronic inflammation occurs with atherosclerosis, which is associated with the accumulation of lipids in the vessel wall and the formation of fibrous tissue [36]. Characteristics of carotid artery plaques such as intraplaque hemorrhage (IPH), a large lipid-rich necrotic core (LRNC), and a thin or ruptured fibrous cap (TRFC) are associated with cerebrovascular symptoms [37]. It is also reported that enlargement of an atherosclerotic artery with outward plaque growth or expansive remodeling, might be an important indicator of high-risk plaque [38,39].

VW-MRI is used to assess the morphology and characteristics of carotid artery plaques [5,40,41]. 2D spin echo T1WI technique used to be applied for intraplaque components of carotid artery plaque [40], however, recent MRI studies reported usefulness of 3D MRI in detection of hyperintensity plaque representing IPH, low intensity plaque representing LRNC, and very low intensity representing calcification

[42] (Figure 1).

Acute ICA occlusion

Acute ICA occlusion usually causes severe long-term consequences [43]. There is no gold standard for differentiating acute from chronic carotid occlusion. Acute extracranial ICA occlusions were certainly defined when the estimated time of occlusion was within 7 days prior to CTA [44]. A ring of contrast enhancement in the carotid wall surrounding a hypodense thrombus in the lumen may help differentiate acute from chronic carotid artery occlusion [44]. On ultrasound examination, a mass arising from the ICA that fills the lumen and oscillates with the cardiac cycle is called an "oscillating thrombus" and is considered a specific finding of acute embolic internal carotid occlusive disease [45-47] (Figure 2).

Chronic ICA occlusion

Chronic ICA occlusion (ICAO) is usually formed based on progressive atherosclerosis at the bifurcation of the carotid artery. Both symptomatic and asymptomatic chronic ICAO patients are at high risk for stroke [48]. As the occlusion duration gets longer, the thrombus gradually becomes fibrotic or calcified, and the

occluded segments of ICA undergoes atrophy. The atherosclerotic lesion typically develops from proximal part. The efficacy of carotid endarterectomy (CEA) has been established in symptomatic patients with moderate and greater stenosis [49].

VW-MRI showed that the cervical and petrous segments of ICA are commonly involved in patients with symptomatic and asymptomatic chronic carotid artery occlusion [50]. VW-MRI also revealed that atrophic ICA lead to decreased ipsilateral-to-contralateral diameter ratios at the cervical and petrous segments of ICA, which reduced endovascular recanalization success [48]. In 9 of 13 patients with symptomatic chronic carotid artery occlusion, VW-MRI showed contrast enhancement of the thrombus [50].

Diagnostic utility of VW-MRI in stroke

VW-MRI has provided supplemental information to luminal imaging [51], but diagnostic utility of VW-MRI in the work-up of ischemic stroke has also been reported. Kesav et al reported that VW-MRI reclassified etiology and influenced diagnostic evaluation in cases originally classified as “undetermined” etiologies and large (intracranial) artery atherosclerosis [52]. Song et al reported that VW-MRI changed etiologic classification, resulting in a higher percentage of cases reclassified as intracranial atherosclerotic disease [51]. VW-MRI can significantly improve diagnostic

differentiation of intracranial vascular disorders compared with luminal imaging alone [51,53,54].

Specifically, vessel wall enhancement is important in diagnostic differentiation. Vessel wall enhancement may be associated with the culprit plaque in acute ischemic stroke. VW-MRI revealed vessel wall enhancement in 28 of 48 patients with acute ischemic stroke or transient ischemia attack [55]. Hyperintense plaques and plaque surface irregularity may predict A-to-A embolic infarction [56]. Meta-analysis of VW-MRI showed plaques were detected in about half of acute ischemic stroke patients with non-stenotic intracranial MRA [57]. Intracranial high-risk plaque with zero or mild stenosis is associated with ischemic stroke and unfavorable outcome [57]. VW-MRI detected peri-thrombus vascular hyperintensity sign, tubular or tortuous hyperintensity surrounding a filling defect (intravascular thrombus), in 49% of acute ischemic stroke patients [58].

The presence and intensity of vessel wall enhancement has been reported to help differentiate reversible cerebral vasoconstriction syndrome (RCVS) from vasculitis and atherosclerosis [54]. Vessel wall enhancement is associated with both acute and future stroke in patients with cerebral amyloid angiopathy [59].

Dissection

Cervical artery dissection (CAD) affects the cervical portion of the internal carotid artery (ICAD), the vertebral artery (VAD), or both. Cervical pain is often seen in VAD, and headache is seen in ICAD and VAD. The incidence of ICAD is estimated to be slightly higher than that of VAD [60]. CAD is a major cause of ischemic stroke in the young, and intramural hematoma detection significantly contributed to acute ischemic stroke pathogenesis in patients with suspected CAD [61,62]. ICA dissection occurs more often in the intracranial segment than in the cervical segment of the carotid artery [63].

Intracranial artery dissection, which is most common in Asia, accounted for up to 67–78% of all cervicocephalic artery dissections [43] (Figure 3). Intracranial artery dissections often affect the posterior circulation, especially at the intradural portion, more frequently than the anterior circulation [64,65]. Intracranial cerebral artery dissection of the anterior circulation was reported to be in relation with cortical subarachnoid hemorrhage (SAH) [66]. Intradural arteries are characterized by a well-developed internal elastic lamina, a paucity of elastic fibers in the media, little adventitial tissue, and no external elastic lamina [67], which may result in weaker supporting tissues than cervical arteries and may be associated with SAH [68]. (Figure 4)

On VW-MRI, intramural hematoma is iso-intensity during acute phase of CAD,

subsequently become hyperintensity a few days after the onset until about 2 months or later. Follow-up imaging is necessary for CAD, and intramural hematoma usually heal within 3-6 months.

Carotid web

A carotid web is a thin intraluminal filling defect along the posterior wall of the carotid bulb observed on CTA or DSA. Carotid web may contribute to recurrent ipsilateral ischemic stroke in patients with no other determined stroke risks [69]. During a 12-month period, ipsilateral carotid webs were identified prospectively in 7 patients with acute ischemic stroke at the single institute [69]. In another series, carotid artery webs were found in 2 of 132 symptomatic patients with suspected stroke and in 7 of 312 asymptomatic patients [70]. Pathological analysis for carotid web showed marked fibroelastic thickening of the intima. Although the incidence of carotid web is low, and CTA is the better tool for detection of carotid web, VW-MRI may depict the presence of carotid web (Figure 5). Neuroradiologists should check the abnormalities of carotid bulb especially in patients with recurrent ipsilateral stroke.

Aneurysm

MRA is suitable for serial follow-up of aneurysms and recent progress of compressed sensing technique enables high resolution MRA with wide coverage in clinical routines [71,72].

Although MRA or CTA can be easily performed and they provide intraluminal characteristics, VW-MRI provides the characteristics of aneurysmal wall. Wall thickening with enhancement was associated with unstable (ruptured, symptomatic, or undergoing morphological modification) intracranial aneurysms [73]. Several mechanisms including inflammatory response, vasa vasorum, atherosclerosis, and intramural hematoma may cause aneurysmal wall enhancement. Whether aneurysmal wall enhancement on VW-MRI represents inflammatory process or not has not been answered yet [74]. Wall enhancement might imply fragility of the aneurysm wall which leads to remodeling, thinning, and daughter sac formation [75]. In terms of the size of aneurysms, wall enhancement was noted on all large aneurysms (≥7 mm) and 67% (20/30) of the small aneurysms (<7 mm) [76].

Angiogram-negative SAH

Angiogram-negative SAH comprises of approximately 15% of SAH case in which no causative vascular abnormality was found on angiography [77]. Angiogram-

negative SAH can be classified into two subgroups: one is perimesencephalic SAH in which distribution of SAH is observed at the perimesencephalic region with low risk of recurrent hemorrhage and excellent clinical outcome. The other is non-perimesencephalic diffuse SAH in which angiogram-negative SAH may develop hydrocephalus, vasospasm, rebleeding, which results in poor clinical outcome due to the presence of undetected vascular abnormalities [78].

Recent retrospective study showed VW-MRI revealed that abnormal findings such as dissection and blood blister-like aneurysm in 14 out of 17 patients with diffuse non-aneurysmal SAH [23].

AVM

Brain AVM is an abnormal connection between arteries and veins existing in the brain parenchyma without intervening capillary beds. The transition between artery and vein is called as a nidus. The risk of hemorrhage is associated with deep venous drainage, and deep and infratentorial brain location [79], and demographically children and females [80]. TOF-MRA with wide coverage like a whole brain MRA is necessary to evaluate feeders and nidus of AVM [81]. CE-MRA or MR-DSA is also performed for evaluation of brain MRA [82].

VW-MRI is also considered important for evaluation of thrombus formation in nidus and the rupture risk of AVM. Comparison of VW-MRI and histopathology findings in a ruptured AVM revealed luminal thrombus in the vessel wall, fibrin deposition inside and outside the vessel, and inflammatory cell infiltration [83]. VW-MRI demonstrates nidal enhancement and perivascular enhancement adjacent to the nidus even in unruptured AVM [84]. Although enhancement on VW-MRI may represent remodeled vessel wall without active inflammation as well as true persistent inflammatory changes, further longitudinal studies are required [84].

Moyamoya disease

3T MRA clearly visualize moyamoya vessels with the advantage of T1 elongation and MT effect [85]. Intraluminal flow is often evaluated with TOF-MRA in moyamoya disease, and recent technical improvement such as compressed sensing enables us to perform TOF MRA with wide coverage [86].

Although initial studies for a small number of cases reported lack or weak contrast enhancement of vessel wall [87,88], recent studies showed a high frequency of ICA and MCA wall enhancement [89]. Another study revealed negative remodeling of the vessels in moyamoya patients [90]. However, most previous studies have focused on

differentiating moyamoya disease from atherosclerotic disease, and only a limited number of studies have focused on the relationship between VW-MRI and the disease activity [91]. Consequently, the clinical usefulness of VW-MRI for moyamoya disease is not established yet.

Reversible cerebral vasoconstriction syndrome (RCVS)

RCVS is characterized by severe headaches, with or without other acute neurological symptoms, and diffuse segmental constriction of cerebral arteries that resolves spontaneously within 3 months [92]. A thunderclap headache is a severe pain that peaks within seconds and usually recurs for one to two weeks [92,93]. Patients typically report at least one trigger such as sexual activity, straining during defecation, stressful or emotional situations, physical exertion, coughing, sneezing, urination, bathing, showering, swimming, laughing, sudden bending down, postpartum state, pre-eclampsia, recreational drugs, vasoactive substances, and antidepressants [92,94].

Imaging abnormalities include cortical SAH, cerebral infarction, intracerebral hemorrhage, and reversible brain edema [92,94]. Diagnostic criteria include the demonstration of segmental vasoconstriction. It is worth noting that even in the presence of hemorrhage or cerebral edema, initial angiogram may be normal if the examination is

performed early and vasoconstriction can be difficult to detect in very distal branches [95,96]. Follow-up examination should be performed several days later for detection of vasoconstriction if RCVS is clinically suspected. VW-MRI of RCVS shows minimal to no enhancement and minimal wall thickening [54]. VW-MRI may help distinguish RCVS from vasculitis and intracranial atherosclerosis.

Clinical application of VW-MRI – Venous disease

Venous structures

Venous structures are usually evaluated with susceptibility-weighted imaging (SWI). SWI is a high spatial resolution three-dimensional (3D) gradient echo MR technique that exploits the magnetic susceptibility differences. SWI shows deoxyhemoglobin inside the veins due to its paramagnetic property [97]. SWI visualize hypointense venous structures in acute large arterial infarction probably due to increase of deoxyhemoglobin and dilatation of veins [98].

VW-MRI is also useful for evaluation of venous structures. The positive findings of venous thrombus used to be non-filling of venous sinus or cerebral vein on CE-CT or CE-MRI. On the other hand, VW-MRI can show the thrombus as evident high signal intensity even in the subacute stage of venous thrombosis without administration of

contrast media [99] (Figure 6).

Clinical application of VW-MRI – Vasculitis

CNS Vasculitis

Adult primary angiitis of the central nervous system (PACNS) is a heterogenous disease although secondary CNS vasculitis is ruled out with complete work-up for malignancies, cardiopathy, systemic vasculitis, and connective tissue disorders. Most of PACNS shows multi-territorial, bilateral, distal acute stroke lesions with small to medium artery distribution, and a predominant carotid artery distribution [100]. Hemorrhagic infarctions and parenchymal hemorrhages were also frequently found [100]. Occasionally PACNS showed tumor-like appearance characterized with mainly small-sized vessel disease mimicking primary CNS lymphoma, however, global outcomes are good under appropriate treatment [101]. Tumor-like PACNS can be seen in younger patients compared with the other PACNS and accompanies seizure, and more enhancement on CE MRI [101].

VW-MRI revealed a concentric contrast enhancement of arterial walls, localized in multiple vascular territories in patient with PACNS [102,103]. According to the systematic review of CNS vasculitis, features of VW-MRI for vasculitis affecting the

intracranial and extracranial arteries included vessel wall enhancement (89%), vessel wall thickening (72%), vessel wall edema (10%), or perivascular enhancement (16%) [104].

Giant cell arteritis (GCA)

GCA or temporal arteritis is the most common idiopathic large vessel vasculitis as well as Takayasu arteritis. Patients are usually greater than 50 years of age and it mainly affects the thoracic and abdominal aorta, and its primary branches. The etiology and pathogenesis of GCA are still unknown. Classic cranial manifestations consist of headache, scalp tenderness, jaw claudication, and vision loss. Vision loss occurs in approximately 20% of patients with GCA and immediate diagnosis and early initiation of intravenous high-dose corticosteroid therapy are required [105]. Stroke or transient ischemic attack occur in 1.5–7% of patients with GCA and are caused by stenosis or occlusion of the extradural vertebral or carotid arteries [106,105]. GCA tends to affect arteries with elastic tissue in their wall, whereas intradural arteries contain little or no elastic tissue. Inflammatory cells enter the vessel wall through vasa vasorum which is less in intradural arteries. These are thought to be the reasons why intracranial lesions of GCA are rare. Temporal artery biopsy remains the gold standard for diagnosis of GCA.

3D VW-MRI increased diagnostic accuracy of GCA compared with 2D VW-

MRI [107]. 18F Fluorodeoxyglucose Positron emission tomography (FDG-PET)/CT is also useful for the diagnosis, therapy response assessment, and prognosis of GCA [108]. Arteritic anterior ischemic optic neuropathy (A-AION) is the most common cause for permanent vision impairment in patients with GCA [105]. A-AION is caused by arteritic ischemia of the anterior part of the optic nerve secondary to inflammatory occlusion of the posterior ciliary arteries. VW-MRI revealed a strong and blurry contrast enhancement aside the optic nerve and the adjacent orbital fat following the course of the posterior ciliary arteries [109].

Other vasculitis and inflammatory diseases

VW-MRI can depict inflammatory changes in a wide range of secondary vasculitis, including radiation-induced and those associated with infectious disease such as the human immunodeficiency virus (HIV), syphilis [110], herpes [111] and varicella zoster (Figure 7). Preliminary findings obtained with VW-MRI also suggested a possible inflammatory mechanism underlying a percentage of cryptogenic stroke in coronavirus disease 2019 (COVID-19) patients [112]. VW-MRI can identify inflamed intracranial vessels, enabling precise localization of biopsy targets [113]. MR findings are important in the management of infectious diseases [114], and VW-MRI may add values in

diagnostic workups.

Clinical application of VW-MRI – Leptomeningeal diseases

Leptomeningeal diseases

Image sequences used for VW-MRI are spin-echo based pulse sequences have relatively lower signal intensity in white matter, in part due to MT effects [115]. In addition, intravascular signal suppression facilitates detection of microscopic metastases and leptomeningeal carcinomatosis [116].

3D CE VW-MRI showed a higher sensitivity than CE gradient echo MRI in detection of leptomeningeal carcinomatosis [117] (Figure 8).

Conclusion

VW-MRI has been applied in clinical practices not only in evaluation of vulnerable plaques, but various kinds of cerebrovascular diseases, vasculitis, and other diseases. High resolution 3D VW-MRI with good SNR has been available with or without additional preparation pulses. VW-MRI in addition to the routine MR imaging protocols may lead to better diagnostic workup when necessary.

References

1. Adams HP, Jr., Bendixen BH, Kappelle LJ, Biller J, Love BB, Gordon DL, Marsh EE, 3rd (1993) Classification of subtype of acute ischemic stroke. Definitions for use in a multicenter clinical trial. TOAST. Trial of Org 10172 in Acute Stroke Treatment. Stroke 24 (1):35-41. doi:10.1161/01.str.24.1.35

2. Ay H, Arsava EM, Andsberg G, Benner T, Brown RD, Jr., Chapman SN, Cole JW, Delavaran H, Dichgans M, Engstrom G, Giralt-Steinhauer E, Grewal RP, Gwinn K, Jern C, Jimenez-Conde J, Jood K, Katsnelson M, Kissela B, Kittner SJ, Kleindorfer DO, Labovitz DL, Lanfranconi S, Lee JM, Lehm M, Lemmens R, Levi C, Li L, Lindgren A, Markus HS, McArdle PF, Melander O, Norrving B, Peddareddygari LR, Pedersen A, Pera J, Rannikmae K, Rexrode KM, Rhodes D, Rich SS, Roquer J, Rosand J, Rothwell PM, Rundek T, Sacco RL, Schmidt R, Schurks M, Seiler S, Sharma P, Slowik A, Sudlow C, Thijs V, Woodfield R, Worrall BB, Meschia JF (2014) Pathogenic ischemic stroke phenotypes in the NINDS-stroke genetics network. Stroke 45 (12):3589-3596. doi:10.1161/STROKEAHA.114.007362

3. Adams HP, Jr., Biller J (2015) Classification of subtypes of ischemic stroke: history of the trial of org 10172 in acute stroke treatment classification. Stroke 46 (5):e114-117. doi:10.1161/STROKEAHA.114.007773

4. Amarenco P, Bogousslavsky J, Caplan LR, Donnan GA, Wolf ME, Hennerici MG (2013) The ASCOD phenotyping of ischemic stroke (Updated ASCO Phenotyping). Cerebrovasc Dis 36 (1):1-5. doi:10.1159/000352050

5. Cappendijk VC, Cleutjens KB, Kessels AG, Heeneman S, Schurink GW, Welten RJ, Mess WH, Daemen MJ, van Engelshoven JM, Kooi ME (2005) Assessment of human atherosclerotic carotid plaque components with multisequence MR imaging: initial experience. Radiology 234 (2):487-492. doi:10.1148/radiol.2342032101

6. Park J, Mugler JP, 3rd, Horger W, Kiefer B (2007) Optimized T1-weighted contrast for single-slab 3D turbo spin-echo imaging with long echo trains: application to whole-brain imaging. Magn Reson Med 58 (5):982-992. doi:10.1002/mrm.21386

7. Fan Z, Zhang Z, Chung YC, Weale P, Zuehlsdorff S, Carr J, Li D (2010) Carotid arterial wall MRI at 3T using 3D variable-flip-angle turbo spin-echo (TSE) with flow-sensitive dephasing (FSD). J Magn Reson Imaging 31 (3):645-654. doi:10.1002/jmri.22058

8. Storey P, Atanasova IP, Lim RP, Xu J, Kim D, Chen Q, Lee VS (2010) Tailoring the flow sensitivity of fast spin-echo sequences for noncontrast peripheral MR angiography. Magn Reson Med 64 (4):1098-1108. doi:10.1002/mrm.22510

9. Henningsson M, Malik S, Botnar R, Castellanos D, Hussain T, Leiner T (2022) Black-Blood Contrast in Cardiovascular MRI. J Magn Reson Imaging 55 (1):61-80.

doi:10.1002/jmri.27399

10. Busse RF, Brau AC, Vu A, Michelich CR, Bayram E, Kijowski R, Reeder SB, Rowley HA (2008) Effects of refocusing flip angle modulation and view ordering in 3D fast spin echo. Magn Reson Med 60 (3):640-649. doi:10.1002/mrm.21680

11. Guggenberger K, Krafft AJ, Ludwig U, Raithel E, Forman C, Meckel S, Hennig J, Bley TA, Vogel P (2021) Intracranial vessel wall imaging framework - Data acquisition, processing, and visualization. Magn Reson Imaging 83:114-124. doi:10.1016/j.mri.2021.08.004

12. Okuchi S, Fushimi Y, Okada T, Yamamoto A, Okada T, Kikuchi T, Yoshida K, Miyamoto S, Togashi K (2019) Visualization of carotid vessel wall and atherosclerotic plaque: T1-SPACE vs. compressed sensing T1-SPACE. Eur Radiol 29 (8):4114-4122. doi:10.1007/s00330-018-5862-8

13. Song JW, Moon BF, Burke MP, Kamesh Iyer S, Elliott MA, Shou H, Messe SR, Kasner SE, Loevner LA, Schnall MD, Kirsch JE, Witschey WR, Fan Z (2020) MR Intracranial Vessel Wall Imaging: A Systematic Review. J Neuroimaging 30 (4):428-442. doi:10.1111/jon.12719

14. Hui FK, Zhu X, Jones SE, Uchino K, Bullen JA, Hussain MS, Lou X, Jiang WJ (2015) Early experience in high-resolution MRI for large vessel occlusions. J Neurointerv Surg

7 (7):509-516. doi:10.1136/neurintsurg-2014-011142

15. Mandell DM, Mossa-Basha M, Qiao Y, Hess CP, Hui F, Matouk C, Johnson MH, Daemen MJ, Vossough A, Edjlali M, Saloner D, Ansari SA, Wasserman BA, Mikulis DJ, Vessel Wall Imaging Study Group of the American Society of N (2017) Intracranial Vessel Wall MRI: Principles and Expert Consensus Recommendations of the American Society of Neuroradiology. AJNR Am J Neuroradiol 38 (2):218-229. doi:10.3174/ajnr.A4893

16. Wang J, Yarnykh VL, Hatsukami T, Chu B, Balu N, Yuan C (2007) Improved suppression of plaque-mimicking artifacts in black-blood carotid atherosclerosis imaging using a multislice motion-sensitized driven-equilibrium (MSDE) turbo spin-echo (TSE) sequence. Magn Reson Med 58 (5):973-981. doi:10.1002/mrm.21385

17. Brown R, Nguyen TD, Spincemaille P, Cham MD, Choi G, Winchester PA, Prince MR, Wang Y (2010) Effect of blood flow on double inversion recovery vessel wall MRI of the peripheral arteries: quantitation with T2 mapping and comparison with flow-insensitive T2-prepared inversion recovery imaging. Magn Reson Med 63 (3):736-744. doi:10.1002/mrm.22227

18. Fan Z, Yang Q, Deng Z, Li Y, Bi X, Song S, Li D (2017) Whole-brain intracranial vessel wall imaging at 3 Tesla using cerebrospinal fluid-attenuated T1-weighted 3D turbo spin echo. Magn Reson Med 77 (3):1142-1150. doi:10.1002/mrm.26201

19. Li L, Miller KL, Jezzard P (2012) DANTE-prepared pulse trains: a novel approach to motion-sensitized and motion-suppressed quantitative magnetic resonance imaging. Magn Reson Med 68 (5):1423-1438. doi:10.1002/mrm.24142

20. Li L, Chai JT, Biasiolli L, Robson MD, Choudhury RP, Handa AI, Near J, Jezzard P (2014) Black-blood multicontrast imaging of carotid arteries with DANTE-prepared 2D and 3D MR imaging. Radiology 273 (2):560-569. doi:10.1148/radiol.14131717

21. Freeman R, Morris GA (2011) The 'DANTE' experiment. Journal of Magnetic Resonance 213 (2):244-246. doi:https://doi.org/10.1016/j.jmr.2011.08.020

22. Tsekos NV, Garwood M, Merkle H, Xu Y, Wilke N, Ugurbil K (1995) Myocardial tagging with B1 insensitive adiabatic DANTE inversion sequences. Magn Reson Med 34 (3):395-401. doi:10.1002/mrm.1910340317

23. Jung HN, Suh SI, Ryoo I, Kim I (2021) Usefulness of 3D High-resolution Vessel Wall MRI in Diffuse Nonaneurysmal SAH Patients. Clin Neuroradiol 31 (4):1071-1081. doi:10.1007/s00062-021-01018-0

24. Jia S, Zhang L, Ren L, Qi Y, Ly J, Zhang N, Li Y, Liu X, Zheng H, Liang D, Chung YC (2020) Joint intracranial and carotid vessel wall imaging in 5 minutes using compressed sensing accelerated DANTE-SPACE. Eur Radiol 30 (1):119-127. doi:10.1007/s00330-019-06366-7

25. Wang J, Helle M, Zhou Z, Bornert P, Hatsukami TS, Yuan C (2016) Joint blood and cerebrospinal fluid suppression for intracranial vessel wall MRI. Magn Reson Med 75 (2):831-838. doi:10.1002/mrm.25667

26. Cogswell PM, Siero JCW, Lants SK, Waddle S, Davis LT, Gilbert G, Hendrikse J, Donahue MJ (2018) Variable impact of CSF flow suppression on quantitative 3.0T intracranial vessel wall measurements. J Magn Reson Imaging 48 (4):1120-1128. doi:10.1002/jmri.26028

27. Taoka T, Naganawa S (2021) Imaging for central nervous system (CNS) interstitial fluidopathy: disorders with impaired interstitial fluid dynamics. Jpn J Radiol 39 (1):1-14. doi:10.1007/s11604-020-01017-0

28. Ishida S, Kimura H, Takei N, Fujiwara Y, Matsuda T, Kanamoto M, Matta Y, Kosaka N, Kidoya E (2021) Separating spin compartments in arterial spin labeling using delays alternating with nutation for tailored excitation (DANTE) pulse: A validation study using T2 -relaxometry and application to arterial cerebral blood volume imaging. Magn Reson Med. doi:10.1002/mrm.29052

29. Kim D, Heo YJ, Jeong HW, Baek JW, Han JY, Lee JY, Jin SC, Baek HJ (2019) Usefulness of the Delay Alternating with Nutation for Tailored Excitation Pulse with T1-Weighted Sampling Perfection with Application-Optimized Contrasts Using Different

Flip Angle Evolution in the Detection of Cerebral Metastases: Comparison with MPRAGE Imaging. AJNR Am J Neuroradiol 40 (9):1469-1475. doi:10.3174/ajnr.A6158

30. Oshima S, Fushimi Y, Okada T, Nakajima S, Yokota Y, Shima A, Grinstead J, Ahn S, Sawamoto N, Takahashi R, Nakamoto Y (2021) Neuromelanin-Sensitive Magnetic Resonance Imaging Using DANTE Pulse. Mov Disord 36 (4):874-882. doi:10.1002/mds.28417

31. Wan L, Zhang N, Zhang L, Long X, Jia S, Li Y, Liang D, Zheng H, Liu X (2019) Reproducibility of simultaneous imaging of intracranial and extracranial arterial vessel walls using an improved T1-weighted DANTE-SPACE sequence on a 3T MR system. Magn Reson Imaging 62:152-158. doi:10.1016/j.mri.2019.04.016

32. Shinohara Y, Takahashi N, Lee Y, Ohmura T, Umetsu A, Kinoshita F, Kuya K, Kato A, Kinoshita T (2020) Usefulness of deep learning-assisted identification of hyperdense MCA sign in acute ischemic stroke: comparison with readers' performance. Jpn J Radiol 38 (9):870-877. doi:10.1007/s11604-020-00986-6

33. Chen L, Zhao H, Jiang H, Balu N, Geleri DB, Chu B, Watase H, Zhao X, Li R, Xu J, Hatsukami TS, Xu D, Hwang JN, Yuan C (2021) Domain adaptive and fully automated carotid artery atherosclerotic lesion detection using an artificial intelligence approach (LATTE) on 3D MRI. Magn Reson Med 86 (3):1662-1673. doi:10.1002/mrm.28794

34. Zhou Z, Chen S, Balu N, Chu B, Zhao X, Sun J, Mossa-Basha M, Hatsukami T, Bornert P, Yuan C (2021) Neural network enhanced 3D turbo spin echo for MR intracranial vessel wall imaging. Magn Reson Imaging 78:7-17. doi:10.1016/j.mri.2021.01.004

35. Lusis AJ (2000) Atherosclerosis. Nature 407 (6801):233-241. doi:10.1038/35025203

36. Ross R (1999) Atherosclerosis--an inflammatory disease. N Engl J Med 340 (2):115-126. doi:10.1056/NEJM199901143400207

37. Kassem M, Florea A, Mottaghy FM, van Oostenbrugge R, Kooi ME (2020) Magnetic resonance imaging of carotid plaques: current status and clinical perspectives. Ann Transl Med 8 (19):1266. doi:10.21037/atm-2020-cass-16

38. Kurosaki Y, Yoshida K, Fukumitsu R, Sadamasa N, Handa A, Chin M, Yamagata S (2016) Carotid artery plaque assessment using quantitative expansive remodeling evaluation and MRI plaque signal intensity. J Neurosurg 124 (3):736-742. doi:10.3171/2015.2.JNS142783

39. Yoshida K, Yang T, Yamamoto Y, Kurosaki Y, Funaki T, Kikuchi T, Ishii A, Kataoka H, Miyamoto S (2019) Expansive carotid artery remodeling: possible marker of vulnerable plaque. J Neurosurg:1-6. doi:10.3171/2019.7.JNS19727

40. Yuan C, Mitsumori LM, Beach KW, Maravilla KR (2001) Carotid atherosclerotic

plaque: noninvasive MR characterization and identification of vulnerable lesions. Radiology 221 (2):285-299. doi:10.1148/radiol.2212001612

41. Yoshida K, Narumi O, Chin M, Inoue K, Tabuchi T, Oda K, Nagayama M, Egawa N, Hojo M, Goto Y, Watanabe Y, Yamagata S (2008) Characterization of carotid atherosclerosis and detection of soft plaque with use of black-blood MR imaging. AJNR Am J Neuroradiol 29 (5):868-874. doi:10.3174/ajnr.A1015

42. Baylam Geleri D, Watase H, Chu B, Chen L, Zhao H, Zhao X, Hatsukami TS, Yuan C, Collaborators C-IS (2022) Detection of Advanced Lesions of Atherosclerosis in Carotid Arteries Using 3-Dimensional Motion-Sensitized Driven-Equilibrium Prepared Rapid Gradient Echo (3D-MERGE) Magnetic Resonance Imaging as a Screening Tool. Stroke 53 (1):194-200. doi:10.1161/STROKEAHA.120.032505

43. Debette S, Compter A, Labeyrie MA, Uyttenboogaart M, Metso TM, Majersik JJ, Goeggel-Simonetti B, Engelter ST, Pezzini A, Bijlenga P, Southerland AM, Naggara O, Bejot Y, Cole JW, Ducros A, Giacalone G, Schilling S, Reiner P, Sarikaya H, Welleweerd JC, Kappelle LJ, de Borst GJ, Bonati LH, Jung S, Thijs V, Martin JJ, Brandt T, Grond-Ginsbach C, Kloss M, Mizutani T, Minematsu K, Meschia JF, Pereira VM, Bersano A, Touze E, Lyrer PA, Leys D, Chabriat H, Markus HS, Worrall BB, Chabrier S, Baumgartner R, Stapf C, Tatlisumak T, Arnold M, Bousser MG (2015) Epidemiology,

pathophysiology, diagnosis, and management of intracranial artery dissection. Lancet Neurol 14 (6):640-654. doi:10.1016/S1474-4422(15)00009-5

44. Michel P, Ntaios G, Delgado MG, Bezerra DC, Meuli R, Binaghi S (2012) CT angiography helps to differentiate acute from chronic carotid occlusion: the "carotid ring sign". Neuroradiology 54 (2):139-146. doi:10.1007/s00234-011-0868-9

45. Tanaka K, Uehara T, Miyoshi M, Miyashita F, Matsuyama TA, Ishibashi-Ueda H, Toyoda K (2013) Oscillating thrombi in bilateral extracranial internal carotid arteries demonstrated on ultrasonography: two autopsy cases of cardioembolic stroke. Intern Med 52 (11):1243-1247. doi:10.2169/internalmedicine.52.9558

46. Kwon SU, Lee SH, Kim JS (2002) Sudden coma from acute bilateral internal carotid artery territory infarction. Neurology 58 (12):1846-1849. doi:10.1212/wnl.58.12.1846

47. Hagiwara N, Toyoda K, Fujimoto S, Okada Y (2003) Extensive bihemispheric ischemia caused by acute occlusion of three major arteries to the brain. J Neurol Sci 212 (1-2):99-101. doi:10.1016/s0022-510x(03)00084-4

48. Yan C, Wang J, Guo R, Jin W, Zhao Y, Wang R (2021) Vascular Diameters as Predictive Factors of Recanalization Surgery Outcomes in Internal Carotid Artery Occlusion. Front Neurol 12:632063. doi:10.3389/fneur.2021.632063

49. Yoshida K, Miyamoto S (2015) Evidence for management of carotid artery stenosis.

Neurol Med Chir (Tokyo) 55 (3):230-240. doi:10.2176/nmc.ra.2014-0361

50. Wan M, Yan L, Xu Z, Hou Z, Kang K, Cui R, Yu Y, Song J, Hui FK, Wang Y, Miao Z, Lou X, Ma N (2022) Symptomatic and Asymptomatic Chronic Carotid Artery Occlusion on High-Resolution MR Vessel Wall Imaging. AJNR Am J Neuroradiol 43 (1):110-116. doi:10.3174/ajnr.A7365

51. Song JW (2019) Impact of Vessel Wall MR Imaging in the Work-Up for Ischemic Stroke. AJNR Am J Neuroradiol 40 (10):1707-1708. doi:10.3174/ajnr.A6241

52. Kesav P, Krishnavadana B, Kesavadas C, Sreedharan SE, Rajendran A, Sukumaran S, Sylaja PN (2019) Utility of intracranial high-resolution vessel wall magnetic resonance imaging in differentiating intracranial vasculopathic diseases causing ischemic stroke. Neuroradiology 61 (4):389-396. doi:10.1007/s00234-019-02157-5

53. Tandon V, Senthilvelan S, Sreedharan SE, Kesavadas C, Vt J, Sylaja PN (2022) High-resolution MR vessel wall imaging in determining the stroke aetiology and risk stratification in isolated middle cerebral artery disease. Neuroradiology. doi:10.1007/s00234-021-02891-9

54. Mossa-Basha M, Hwang WD, De Havenon A, Hippe D, Balu N, Becker KJ, Tirschwell DT, Hatsukami T, Anzai Y, Yuan C (2015) Multicontrast high-resolution vessel wall magnetic resonance imaging and its value in differentiating intracranial

vasculopathic processes. Stroke 46 (6):1567-1573. doi:10.1161/STROKEAHA.115.009037

55. Woo NE, Na HK, Heo JH, Nam HS, Choi JK, Ahn SS, Choi HS, Lee SK, Lee HS, Cha J, Kim YD (2020) Factors for Enhancement of Intracranial Atherosclerosis in High Resolution Vessel Wall MRI in Ischemic Stroke Patients. Front Neurol 11:580. doi:10.3389/fneur.2020.00580

56. Wu F, Song H, Ma Q, Xiao J, Jiang T, Huang X, Bi X, Guo X, Li D, Yang Q, Ji X, Fan Z, Investigators W (2018) Hyperintense Plaque on Intracranial Vessel Wall Magnetic Resonance Imaging as a Predictor of Artery-to-Artery Embolic Infarction. Stroke 49 (4):905-911. doi:10.1161/STROKEAHA.117.020046

57. Wang Y, Liu X, Wu X, Degnan AJ, Malhotra A, Zhu C (2019) Culprit intracranial plaque without substantial stenosis in acute ischemic stroke on vessel wall MRI: A systematic review. Atherosclerosis 287:112-121. doi:10.1016/j.atherosclerosis.2019.06.907

58. Chen Q, Wang W, Chen YC, Chen G, Ni L, Zhang D, Zhou J, Yin XD (2020) Peri-thrombus vascular hyperintensity sign: detection of intracranial thrombus location and length in acute ischemic stroke. Jpn J Radiol 38 (6):516-523. doi:10.1007/s11604-020-00937-1

59. McNally JS, Sakata A, Alexander MD, Dewitt LD, Sonnen JA, Menacho ST, Stoddard GJ, Kim SE, de Havenon AH (2021) Vessel Wall Enhancement on Black-Blood MRI Predicts Acute and Future Stroke in Cerebral Amyloid Angiopathy. AJNR Am J Neuroradiol 42 (6):1038-1045. doi:10.3174/ajnr.A7047

60. Lee VH, Brown RD, Jr., Mandrekar JN, Mokri B (2006) Incidence and outcome of cervical artery dissection: a population-based study. Neurology 67 (10):1809-1812. doi:10.1212/01.wnl.0000244486.30455.71

61. Ducrocq X, Lacour JC, Debouverie M, Bracard S, Girard F, Weber M (1999) [Cerebral ischemic accidents in young subjects. A prospective study of 296 patients aged 16 to 45 years]. Rev Neurol (Paris) 155 (8):575-582

62. McNally JS, Hinckley PJ, Sakata A, Eisenmenger LB, Kim SE, De Havenon AH, Quigley EP, Iacob E, Treiman GS, Parker DL (2018) Magnetic Resonance Imaging and Clinical Factors Associated With Ischemic Stroke in Patients Suspected of Cervical Artery Dissection. Stroke 49 (10):2337-2344. doi:10.1161/STROKEAHA.118.021868

63. Habs M, Pfefferkorn T, Cyran CC, Grimm J, Rominger A, Hacker M, Opherk C, Reiser MF, Nikolaou K, Saam T (2011) Age determination of vessel wall hematoma in spontaneous cervical artery dissection: a multi-sequence 3T cardiovascular magnetic resonance study. J Cardiovasc Magn Reson 13:76. doi:10.1186/1532-429X-13-76

64. Debette S, Leys D (2009) Cervical-artery dissections: predisposing factors, diagnosis, and outcome. Lancet Neurol 8 (7):668-678. doi:10.1016/S1474-4422(09)70084-5

65. Mehdi E, Aralasmak A, Toprak H, Yildiz S, Kurtcan S, Kolukisa M, Asil T, Alkan A (2018) Craniocervical Dissections: Radiologic Findings, Pitfalls, Mimicking Diseases: A Pictorial Review. Curr Med Imaging Rev 14 (2):207-222. doi:10.2174/1573405613666170403102235

66. Fukuma K, Ihara M, Tanaka T, Morita Y, Toyoda K, Nagatsuka K (2015) Intracranial Cerebral Artery Dissection of Anterior Circulation as a Cause of Convexity Subarachnoid Hemorrhage. Cerebrovasc Dis 40 (1-2):45-51. doi:10.1159/000430945

67. Lee RM (1995) Morphology of cerebral arteries. Pharmacol Ther 66 (1):149-173. doi:10.1016/0163-7258(94)00071-a

68. Chen M, Caplan L (2005) Intracranial dissections. Front Neurol Neurosci 20:160-173. doi:10.1159/000088166

69. Choi PM, Singh D, Trivedi A, Qazi E, George D, Wong J, Demchuk AM, Goyal M, Hill MD, Menon BK (2015) Carotid Webs and Recurrent Ischemic Strokes in the Era of CT Angiography. AJNR Am J Neuroradiol 36 (11):2134-2139. doi:10.3174/ajnr.A4431

70. Yang T, Yoshida K, Maki T, Fushimi Y, Yamada K, Okawa M, Yamamoto Y, Takayama N, Suzuki K, Miyamoto S (2021) Prevalence and site of predilection of carotid webs

focusing on symptomatic and asymptomatic Japanese patients. J Neurosurg:1-7. doi:10.3171/2020.8.JNS201727

71. Fushimi Y, Fujimoto K, Okada T, Yamamoto A, Tanaka T, Kikuchi T, Miyamoto S, Togashi K (2016) Compressed Sensing 3-Dimensional Time-of-Flight Magnetic Resonance Angiography for Cerebral Aneurysms: Optimization and Evaluation. Invest Radiol 51 (4):228-235. doi:10.1097/rli.0000000000000226

72. Fushimi Y, Okada T, Kikuchi T, Yamamoto A, Okada T, Yamamoto T, Schmidt M, Yoshida K, Miyamoto S, Togashi K (2017) Clinical evaluation of time-of-flight MR angiography with sparse undersampling and iterative reconstruction for cerebral aneurysms. NMR Biomed 30 (11). doi:10.1002/nbm.3774

73. Edjlali M, Gentric JC, Regent-Rodriguez C, Trystram D, Hassen WB, Lion S, Nataf F, Raymond J, Wieben O, Turski P, Meder JF, Oppenheim C, Naggara O (2014) Does aneurysmal wall enhancement on vessel wall MRI help to distinguish stable from unstable intracranial aneurysms? Stroke 45 (12):3704-3706. doi:10.1161/STROKEAHA.114.006626

74. Cornelissen BMW, Leemans EL, Slump CH, Marquering HA, Majoie C, van den Berg R (2019) Vessel wall enhancement of intracranial aneurysms: fact or artifact? Neurosurg Focus 47 (1):E18. doi:10.3171/2019.4.FOCUS19236

75. Matsushige T, Shimonaga K, Mizoue T, Hosogai M, Hashimoto Y, Takahashi H, Kaneko M, Ono C, Ishii D, Sakamoto S, Kurisu K (2019) Lessons from Vessel Wall Imaging of Intracranial Aneurysms: New Era of Aneurysm Evaluation beyond Morphology. Neurol Med Chir (Tokyo) 59 (11):407-414. doi:10.2176/nmc.ra.2019-0103

76. Tian B, Toossi S, Eisenmenger L, Faraji F, Ballweber MK, Josephson SA, Haraldsson H, Zhu C, Ahn S, Laub G, Hess C, Saloner D (2019) Visualizing wall enhancement over time in unruptured intracranial aneurysms using 3D vessel wall imaging. J Magn Reson Imaging 50 (1):193-200. doi:10.1002/jmri.26553

77. van Gijn J, Rinkel GJ (2001) Subarachnoid haemorrhage: diagnosis, causes and management. Brain 124 (Pt 2):249-278. doi:10.1093/brain/124.2.249

78. Paez-Granda D, Parrilla G, Diaz-Perez J, Espinosa de Rueda M, Garcia-Villalba B, Zamarro J (2021) Are modified Fisher Scale and bleeding pattern helpful predictors of neurological complications in non-aneurysmal subarachnoid hemorrhage? Neuroradiology 63 (2):253-257. doi:10.1007/s00234-020-02524-7

79. Abecassis IJ, Xu DS, Batjer HH, Bendok BR (2014) Natural history of brain arteriovenous malformations: a systematic review. Neurosurg Focus 37 (3):E7. doi:10.3171/2014.6.FOCUS14250

80. Rutledge WC, Ko NU, Lawton MT, Kim H (2014) Hemorrhage rates and risk factors

in the natural history course of brain arteriovenous malformations. Transl Stroke Res 5 (5):538-542. doi:10.1007/s12975-014-0351-0

81. Sakata A, Fushimi Y, Okada T, Nakajima S, Hinoda T, Speier P, Schmidt M, Forman C, Yoshida K, Kataoka H, Miyamoto S, Nakamoto Y (2021) Evaluation of cerebral arteriovenous shunts: a comparison of parallel imaging time-of-flight magnetic resonance angiography (TOF-MRA) and compressed sensing TOF-MRA to digital subtraction angiography. Neuroradiology 63 (6):879-887. doi:10.1007/s00234-020-02581-y

82. Sakata A, Sakamoto R, Fushimi Y, Nakajima S, Hinoda T, Oshima S, Wetzl J, Schmidt M, Okawa M, Yoshida K, Miyamoto S, Nakamoto Y (2022) Low-dose contrast-enhanced time-resolved angiography with stochastic trajectories with iterative reconstruction (IT-TWIST-MRA) in brain arteriovenous shunt. Eur Radiol. doi:10.1007/s00330-022-08678-7

83. Komatsu K, Takagi Y, Ishii A, Kikuchi T, Yamao Y, Fushimi Y, Grinstead J, Ahn S, Miyamoto S (2018) Ruptured intranidal aneurysm of an arteriovenous malformation diagnosed by delay alternating with nutation for tailored excitation (DANTE)-prepared contrast-enhanced magnetic resonance imaging. Acta Neurochir (Wien) 160 (12):2435-2438. doi:10.1007/s00701-018-3713-7

84. Eisenmenger LB, Junn JC, Cooke D, Hetts S, Zhu C, Johnson KM, Manunga JM,

Saloner D, Hess C, Kim H (2021) Presence of Vessel Wall Hyperintensity in Unruptured Arteriovenous Malformations on Vessel Wall Magnetic Resonance Imaging: Pilot Study of AVM Vessel Wall "Enhancement". Front Neurosci 15:697432. doi:10.3389/fnins.2021.697432

85. Fushimi Y, Miki Y, Kikuta K, Okada T, Kanagaki M, Yamamoto A, Nozaki K, Hashimoto N, Hanakawa T, Fukuyama H, Togashi K (2006) Comparison of 3.0- and 1.5-T three-dimensional time-of-flight MR angiography in moyamoya disease: preliminary experience. Radiology 239 (1):232-237. doi:10.1148/radiol.2383042020

86. Yamamoto T, Okada T, Fushimi Y, Yamamoto A, Fujimoto K, Okuchi S, Fukutomi H, Takahashi JC, Funaki T, Miyamoto S, Stalder AF, Natsuaki Y, Speier P, Togashi K (2018) Magnetic resonance angiography with compressed sensing: An evaluation of moyamoya disease. PLoS One 13 (1):e0189493. doi:10.1371/journal.pone.0189493

87. Aoki S, Hayashi N, Abe O, Shirouzu I, Ishigame K, Okubo T, Nakagawa K, Ohtomo K, Araki T (2002) Radiation-induced Arteritis: Thickened Wall with Prominent Enhancement on Cranial MR Images—Report of Five Cases and Comparison with 18 Cases of Moyamoya Disease. Radiology 223 (3):683-688. doi:10.1148/radiol.2233010822

88. Swartz RH, et al. (2009) Intracranial arterial wall imaging using high-resolution 3-

tesla contrast-enhanced MRI. Neurology 72 (7). doi:10.1212/01.wnl.0000342470.69739.b3

89. Ryoo S, Cha J, Kim SJ, Choi JW, Ki C-S, Kim KH, Jeon P, Kim J-S, Hong S-C, Bang OY (2014) High-Resolution Magnetic Resonance Wall Imaging Findings of Moyamoya Disease. Stroke 45 (8):2457-2460. doi:10.1161/strokeaha.114.004761

90. Kaku Y, Morioka M, Ohmori Y, Kawano T, Kai Y, Fukuoka H, Hirai T, Yamashita Y, Kuratsu J-I (2012) Outer-diameter narrowing of the internal carotid and middle cerebral arteries in moyamoya disease detected on 3D constructive interference in steady-state MR image: is arterial constrictive remodeling a major pathogenesis? Acta Neurochir 154 (12):2151-2157. doi:10.1007/s00701-012-1472-4

91. Roder C, Hauser T-K, Ernemann U, Tatagiba M, Khan N, Bender B (2020) Arterial wall contrast enhancement in progressive moyamoya disease. J Neurosurg 132 (6):1845-1853. doi:10.3171/2019.2.jns19106

92. Ducros A (2012) Reversible cerebral vasoconstriction syndrome. Lancet Neurol 11 (10):906-917. doi:10.1016/S1474-4422(12)70135-7

93. Calabrese LH, Dodick DW, Schwedt TJ, Singhal AB (2007) Narrative review: reversible cerebral vasoconstriction syndromes. Ann Intern Med 146 (1):34-44. doi:10.7326/0003-4819-146-1-200701020-00007

94. Caria F, Zedde M, Gamba M, Bersano A, Rasura M, Adami A, Piantadosi C, Quartuccio L, Azzini C, Melis M, Luisa Delodovici M, Dallocchio C, Gandolfo C, Cerrato P, Motto C, Melis F, Chiti A, Gentile M, Bignamini V, Morotti A, Maria Lotti E, Toriello A, Costa P, Silvestrelli G, Zini A, De Giuli V, Poli L, Paciaroni M, Lodigiani C, Marcheselli S, Sanguigni S, Del Sette M, Monaco S, Lochner P, Zanferrari C, Anticoli S, Padovani A, Pezzini A, Italian Project on Stroke at Young Age I (2019) The clinical spectrum of reversible cerebral vasoconstriction syndrome: The Italian Project on Stroke at Young Age (IPSYS). Cephalalgia 39 (10):1267-1276. doi:10.1177/0333102419849013

95. Burton TM, Bushnell CD (2019) Reversible Cerebral Vasoconstriction Syndrome. Stroke 50 (8):2253-2258. doi:10.1161/STROKEAHA.119.024416

96. Ducros A, Fiedler U, Porcher R, Boukobza M, Stapf C, Bousser MG (2010) Hemorrhagic manifestations of reversible cerebral vasoconstriction syndrome: frequency, features, and risk factors. Stroke 41 (11):2505-2511. doi:10.1161/STROKEAHA.109.572313

97. Fushimi Y, Miki Y, Mori N, Okada T, Urayama S, Fukuyama H, Togashi K (2010) Signal changes in the brain on susceptibility-weighted imaging under reduced cerebral blood flow: a preliminary study. J Neuroimaging 20 (3):255-259. doi:10.1111/j.1552-6569.2008.00348.x

98. Kim YW, Choi YY, Park SY, Kim HJ, Kim YS (2021) Prominent hypointense vessel on susceptibility-weighted images accompanying hyperacute and acute large infarction. Jpn J Radiol 39 (7):681-689. doi:10.1007/s11604-021-01107-7

99. Niu PP, Yu Y, Guo ZN, Jin H, Liu Y, Zhou HW, Yang Y (2016) Diagnosis of non-acute cerebral venous thrombosis with 3D T1-weighted black blood sequence at 3T. J Neurol Sci 367:46-50. doi:10.1016/j.jns.2016.05.052

100. Boulouis G, de Boysson H, Zuber M, Guillevin L, Meary E, Costalat V, Pagnoux C, Naggara O, French Vasculitis G (2017) Primary Angiitis of the Central Nervous System: Magnetic Resonance Imaging Spectrum of Parenchymal, Meningeal, and Vascular Lesions at Baseline. Stroke 48 (5):1248-1255. doi:10.1161/STROKEAHA.116.016194

101. de Boysson H, Boulouis G, Dequatre N, Godard S, Neel A, Arquizan C, Detante O, Bloch-Queyrat C, Zuber M, Touze E, Bienvenu B, Aouba A, Guillevin L, Naggara O, Pagnoux C, French Vasculitis Study G (2016) Tumor-Like Presentation of Primary Angiitis of the Central Nervous System. Stroke 47 (9):2401-2404. doi:10.1161/STROKEAHA.116.013917

102. Destrebecq V, Sadeghi N, Lubicz B, Jodaitis L, Ligot N, Naeije G (2020) Intracranial Vessel Wall MRI in Cryptogenic Stroke and Intracranial Vasculitis. J Stroke Cerebrovasc Dis 29 (5):104684. doi:10.1016/j.jstrokecerebrovasdis.2020.104684

103. Mazzacane F, Mazzoleni V, Scola E, Mancini S, Lombardo I, Busto G, Rognone E, Pichiecchio A, Padovani A, Morotti A, Fainardi E (2022) Vessel Wall Magnetic Resonance Imaging in Cerebrovascular Diseases. Diagnostics (Basel) 12 (2). doi:10.3390/diagnostics12020258

104. Arnett N, Pavlou A, Burke MP, Cucchiara BL, Rhee RL, Song JW (2022) Vessel wall MR imaging of central nervous system vasculitis: a systematic review. Neuroradiology 64 (1):43-58. doi:10.1007/s00234-021-02724-9

105. Soriano A, Muratore F, Pipitone N, Boiardi L, Cimino L, Salvarani C (2017) Visual loss and other cranial ischaemic complications in giant cell arteritis. Nat Rev Rheumatol 13 (8):476-484. doi:10.1038/nrrheum.2017.98

106. Samson M, Jacquin A, Audia S, Daubail B, Devilliers H, Petrella T, Martin L, Durier J, Besancenot JF, Lorcerie B, Giroud M, Bonnotte B, Béjot Y (2015) Stroke associated with giant cell arteritis: a population-based study. J Neurol Neurosurg Psychiatry 86 (2):216-221. doi:10.1136/jnnp-2014-307614

107. Poillon G, Collin A, Benhamou Y, Clavel G, Savatovsky J, Pinson C, Zuber K, Charbonneau F, Vignal C, Picard H, Leturcq T, Miranda S, Sene T, Gerardin E, Lecler A (2020) Increased diagnostic accuracy of giant cell arteritis using three-dimensional fat-saturated contrast-enhanced vessel-wall magnetic resonance imaging at 3 T. Eur Radiol

30 (4):1866-1875. doi:10.1007/s00330-019-06536-7

108. Tateishi U, Tsuchiya J, Yokoyama K (2021) Large vessel vasculitis: imaging standards of (18)F-FDG PET/CT. Jpn J Radiol 39 (3):225-232. doi:10.1007/s11604-020-01059-4

109. Sommer NN, Treitl KM, Coppenrath E, Kooijman H, Dechant C, Czihal M, Kolben TM, Beyer SE, Sommer WH, Saam T (2018) Three-Dimensional High-Resolution Black-Blood Magnetic Resonance Imaging for Detection of Arteritic Anterior Ischemic Optic Neuropathy in Patients With Giant Cell Arteritis. Invest Radiol 53 (11):698-704. doi:10.1097/RLI.0000000000000500

110. Zhang K, Chu F, Wang C, Shi M, Yang Y (2021) Progressive Stroke Caused by Neurosyphilis With Concentric Enhancement in the Internal Cerebral Artery on High-Resolution Magnetic Resonance Imaging: A Case Report. Front Neurol 12:675083. doi:10.3389/fneur.2021.675083

111. Tsubouchi R, Ohira J, Sawamura M, Fushimi Y, Grinstead J, Ahn S, Maki T, Takahashi R (2020) Multiple cranial neuritis depicted with DANTE-prepared contrast-enhanced MRI. Neurology and Clinical Neuroscience 8 (4):220-221. doi:https://doi.org/10.1111/ncn3.12400

112. Keller E, Brandi G, Winklhofer S, Imbach LL, Kirschenbaum D, Frontzek K, Steiger

P, Dietler S, Haeberlin M, Willms J, Porta F, Waeckerlin A, Huber M, Abela IA, Lutterotti A, Stippich C, Globas C, Varga Z, Jelcic I (2020) Large and Small Cerebral Vessel Involvement in Severe COVID-19: Detailed Clinical Workup of a Case Series. Stroke 51 (12):3719-3722. doi:10.1161/STROKEAHA.120.031224

113. Zeiler SR, Qiao Y, Pardo CA, Lim M, Wasserman BA (2018) Vessel Wall MRI for Targeting Biopsies of Intracranial Vasculitis. AJNR Am J Neuroradiol 39 (11):2034-2036. doi:10.3174/ajnr.A5801

114. Masuoka S, Miyazaki O, Takahashi H, Tsutsumi Y, Hiyama T, Kitamura M, Okamoto R, Miyasaka M, Minami M, Nosaka S (2021) Predisposing conditions for bacterial meningitis in children: what radiologists need to know. Jpn J Radiol. doi:10.1007/s11604-021-01191-9

115. Kaufmann TJ, Smits M, Boxerman J, Huang R, Barboriak DP, Weller M, Chung C, Tsien C, Brown PD, Shankar L, Galanis E, Gerstner E, van den Bent MJ, Burns TC, Parney IF, Dunn G, Brastianos PK, Lin NU, Wen PY, Ellingson BM (2020) Consensus recommendations for a standardized brain tumor imaging protocol for clinical trials in brain metastases. Neuro Oncol 22 (6):757-772. doi:10.1093/neuonc/noaa030

116. Oh J, Choi SH, Lee E, Shin DJ, Jo SW, Yoo RE, Kang KM, Yun TJ, Kim JH, Sohn CH (2018) Application of 3D Fast Spin-Echo T1 Black-Blood Imaging in the Diagnosis

and Prognostic Prediction of Patients with Leptomeningeal Carcinomatosis. AJNR Am J Neuroradiol 39 (8):1453-1459. doi:10.3174/ajnr.A5721

117. Yoon BC, Saad AF, Rezaii P, Wintermark M, Zaharchuk G, Iv M (2018) Evaluation of Thick-Slab Overlapping MIP Images of Contrast-Enhanced 3D T1-Weighted CUBE for Detection of Intracranial Metastases: A Pilot Study for Comparison of Lesion Detection, Interpretation Time, and Sensitivity with Nonoverlapping CUBE MIP, CUBE, and Inversion-Recovery-Prepared Fast-Spoiled Gradient Recalled Brain Volume. AJNR Am J Neuroradiol 39 (9):1635-1642. doi:10.3174/ajnr.A5747

Figure legends

Figure 1

A 75-year-old male with right ICA stenosis. (a) TOF-MRA shows stenosis of the proximal part of right ICA (arrow). (b) Axial MPR section of DANTE T1-SPACE shows hyperintensity plaque at the right ICA (arrow). (c) Coronal MPR section of DANTE T1-SPACE shows hyperintensity plaque at the right ICA (arrow).

Figure 2

A 75-year-old male with acute onset left hemiparesis. (a) DWI shows hyperintensity in the right internal capsule (black arrow). (b) TOF-MRA shows no apparent inflow inside the right ICA (arrowheads). (c, d, e) 3D T1-SPACE shows intermediated signal inside the right ICA with slight hyperintense structure along the ICA wall (white arrows). Ultrasound shows mobile thrombus or oscillating thrombus in the right ICA (data not shown).

Figure 3

A 45-year-old male with right ICA dissection. The images of 40 days after the onset (a,

c), and 90 days (b, d) are shown: DANTE T1-SPACE (a, b) and TOF-MRA (c, d). (a) DANTE T1-SPACE shows hyperintensity in the false lumen, which represents the intramural thrombosis. (b) DANTE T1-SPACE obtained at 90 days after the onset showed that hyperintensity in the false lumen had regressed. (c) TOF-MRA showed inflow only in the true lumen. (d) The size of true lumen returned to normal at 90 days after the onset.

Figure 4

A 55-year-old female with temporal right hemiparesis. (a) DWI showed hyperintensity in the medial part of right frontal lobe (arrow). DWI also showed widespread hyperintensity in the medial aspect of right frontal lobe (data not shown). (b) MIP image of TOF-MRA shows discontinuous flow in the right ACA (arrowheads). (c) DANTE T1-SPACE showed high intensity spot at the right ACA indicating the thrombosis in the false lumen (arrow). (d) Source image of TOF-MRA showed a slow flow in the true lumen of right ACA (arrow). Acute stroke associated with dissection of right ACA was diagnosed. RCVS was also suspected because of thunderclap headache at onset. However, the stenosis of the right ACA did not improve over time.

Figure 5

A male in his 50 years without any risk factor of atherosclerosis. He suffered from recurrent multiple small brain infarcts in the ipsilateral hemisphere. (a) CE-CTA shows the defect at the proximal part of right ICA (arrow). Carotid web was diagnosed. (b) Non-enhanced MRA shows no apparent abnormality (arrow). (c) Non-enhanced DANTE T1-SPACE showed intermediate signal at right ICA (arrow). (d) Contrast-enhanced DANTE T1-SPACE showed a thin septum projecting into the lumen of right ICA.

Figure 6

A 35 years-old male with venous infarction associated with the venous thrombosis of superficial cerebral vein and the vein of Labbé. (a, b) DANTE T1-SPACE showed hyperintensity in the thrombosed venous structures (arrowheads) as well as the venous hemorrhagic infarction in right temporal lobe (arrow). (c) A thin slice maximum intensity projection image of DANTE T1-SPACE clearly visualized thrombosed vein.

Figure 7

A 60-year-old male with right facial nerve palsy and neuralgia. CE DANTE T1-SPACE (a, c) and CE GRE T1WI (b, d) are shown. He was diagnosed as Ramsay-Hunt syndrome, and CSF analysis demonstrated varicella zoster meningitis. (a, c) CE DANTE T1-SPACE

showed enhancement of right facial nerve and geniculate ganglion (arrows). (b, d) CE GRE T1WI showed less pronounced enhancement in the facial nerve (arrows). Note that non-specific mild enhancement is often seen in geniculate ganglion, but the enhancement is more pronounced in this case.

Figure 8

A 10-year-old girl with CNS dissemination of acute lymphocytic leukemia. CE DANTE T1-SPACE showed enhancement of bilateral vestibular nerves (white arrows), abducens nerves (white arrowheads) (a), trigeminal nerves (black arrows) (b), and oculomotor nerves (white double arrows) (c). CE DANTE T1-SPACE showed leptomeningeal enhancement at the left occipital lobe (black arrowheads) (a, b).

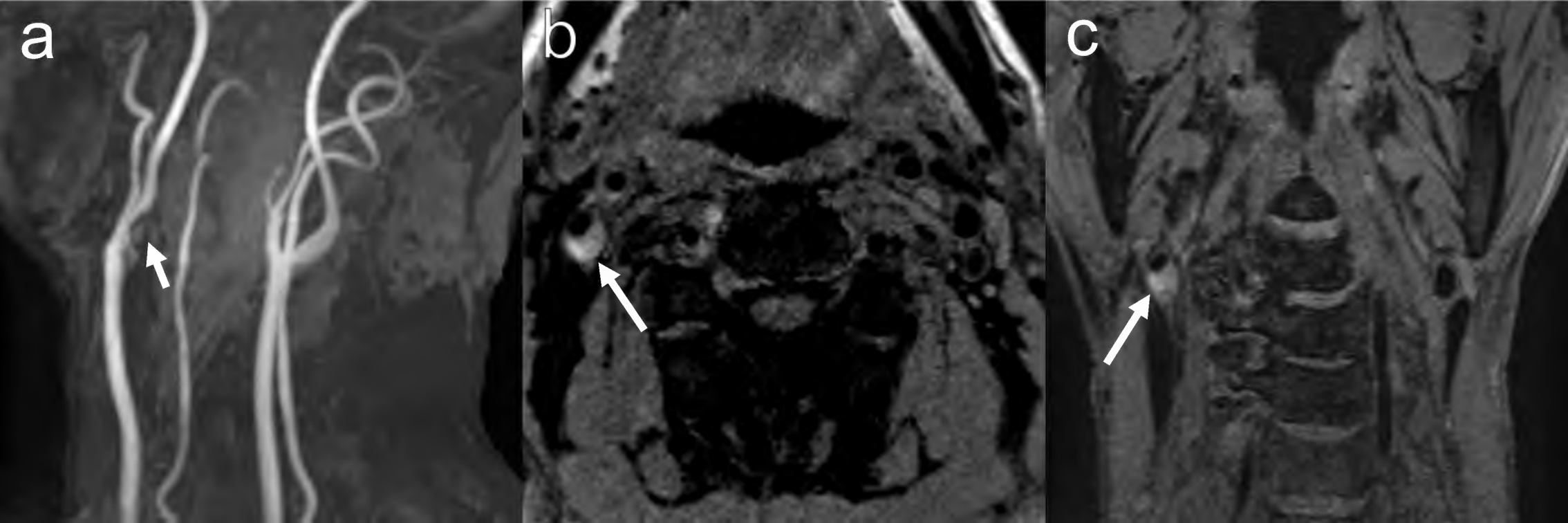
a
b
c

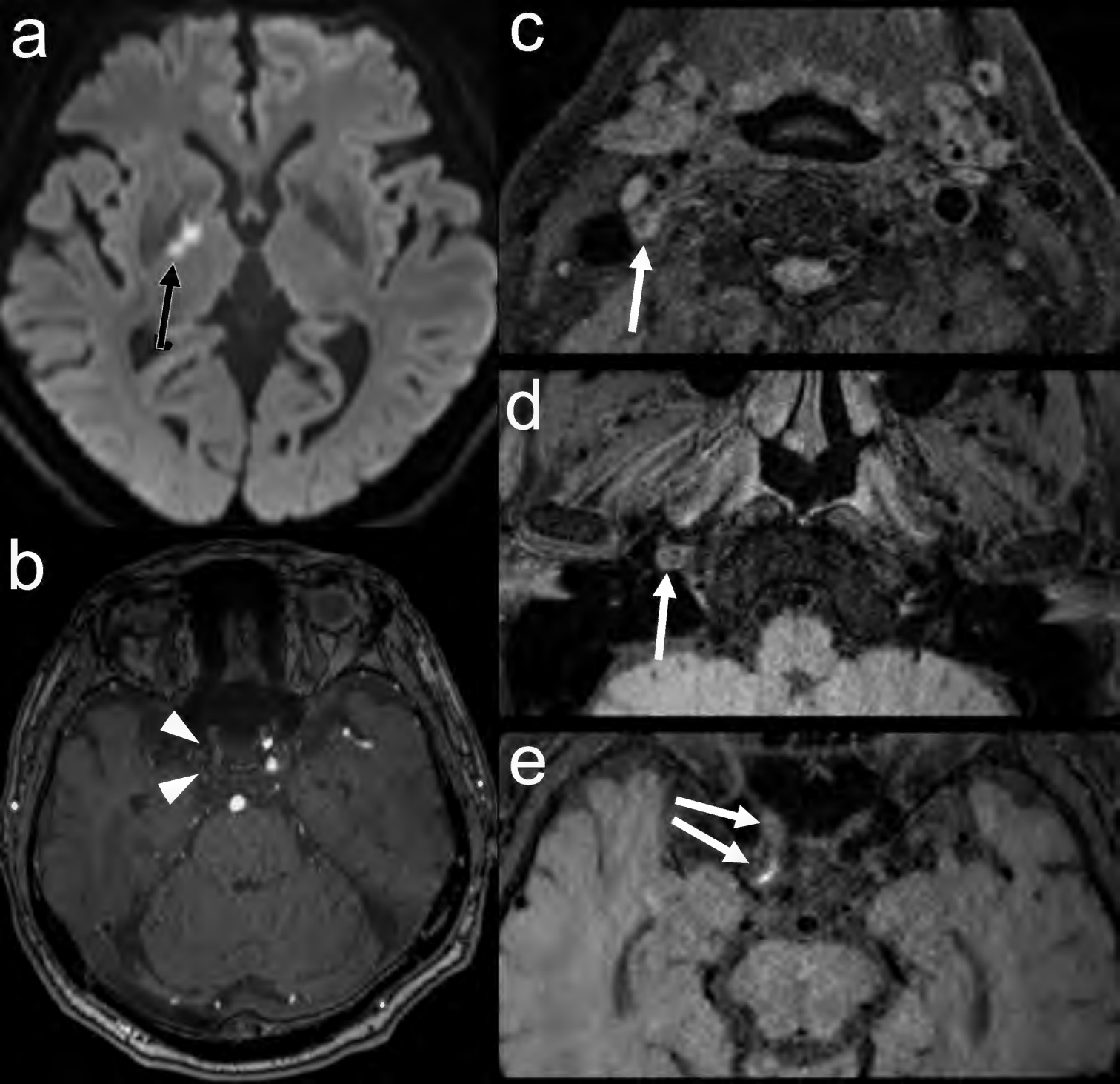
a
b
c
d
e

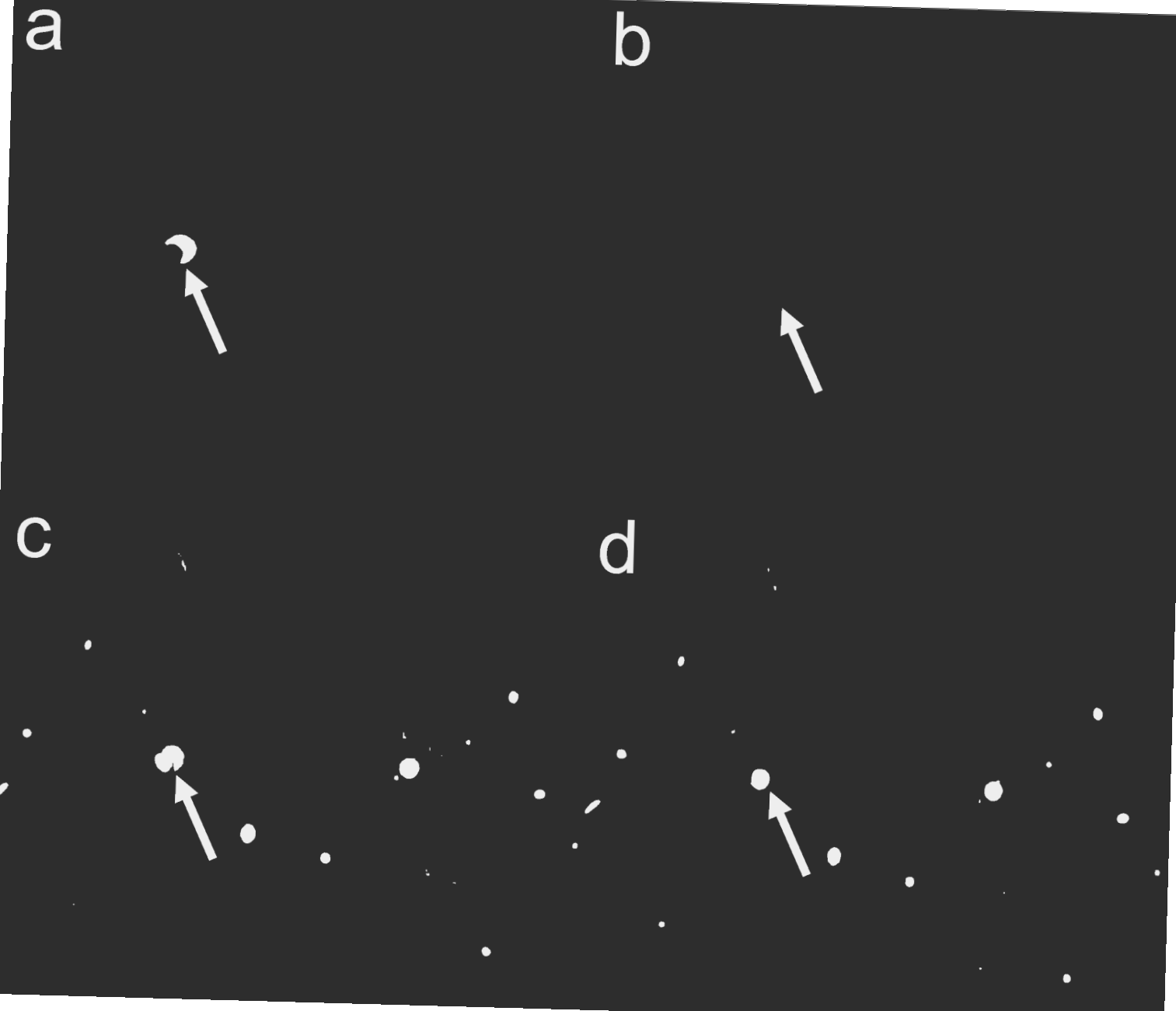
a
b
c
d

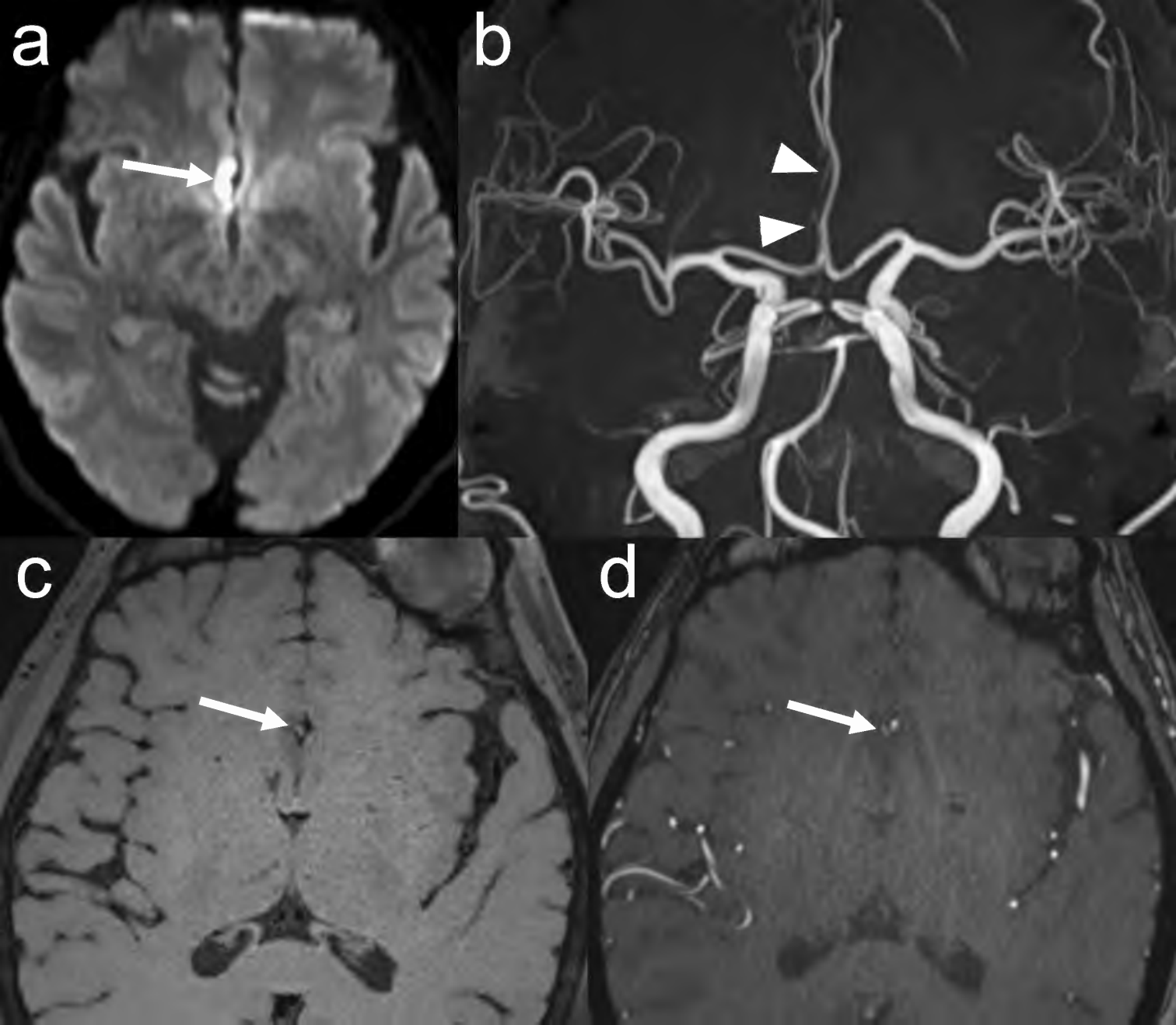
a
b
c
d

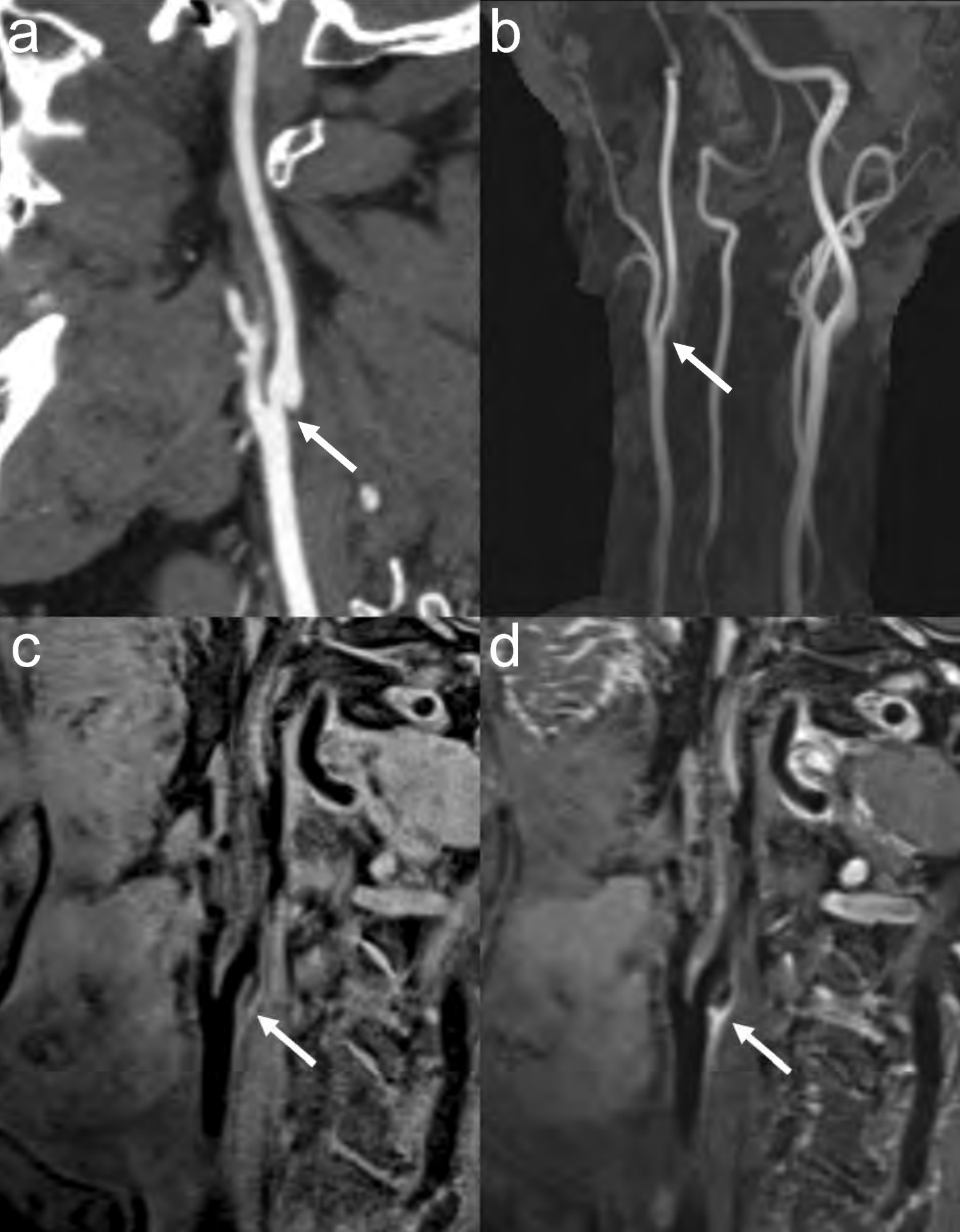
a
b
c
d

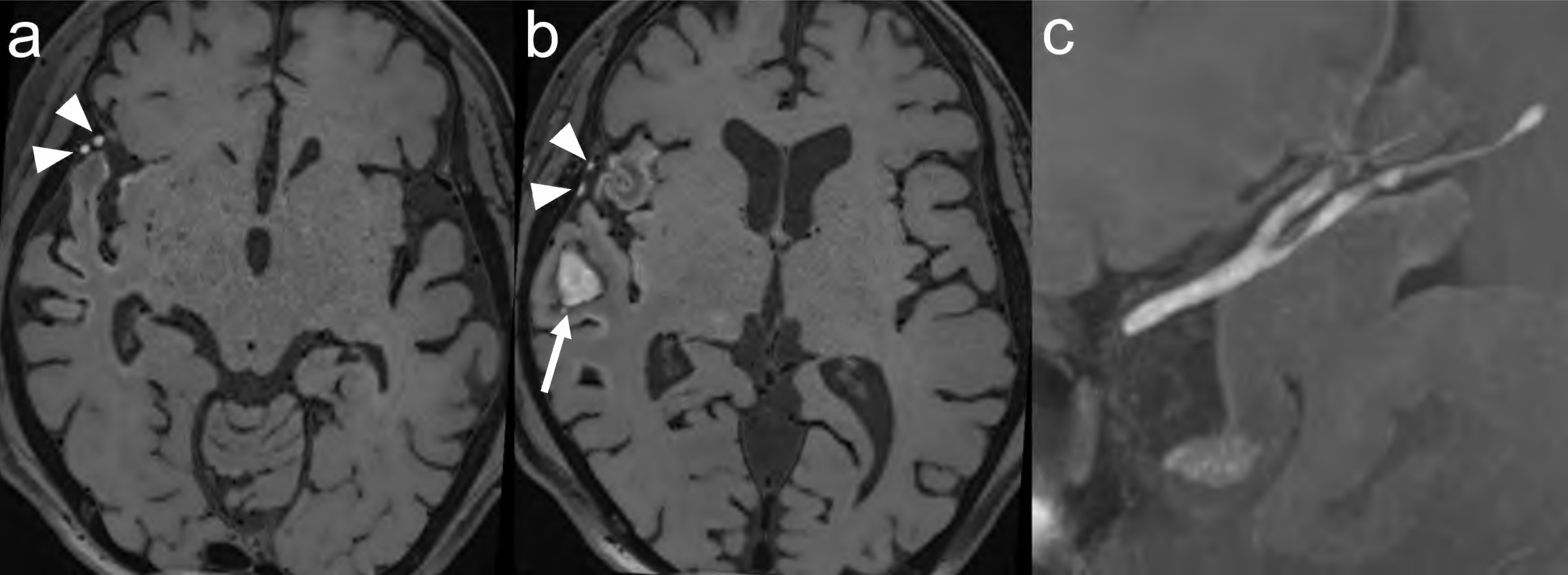
a
b
c

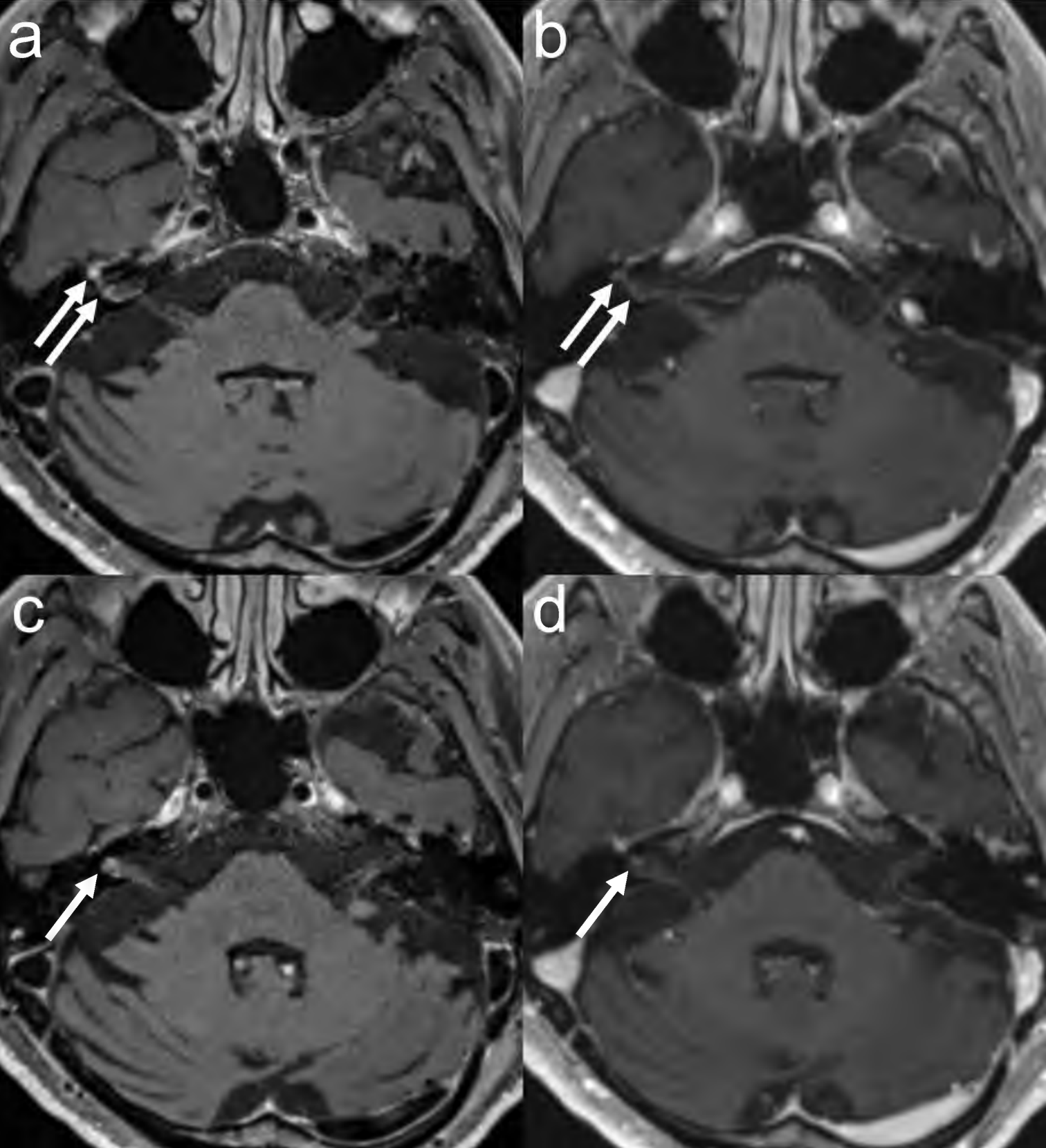
a
b
c
d

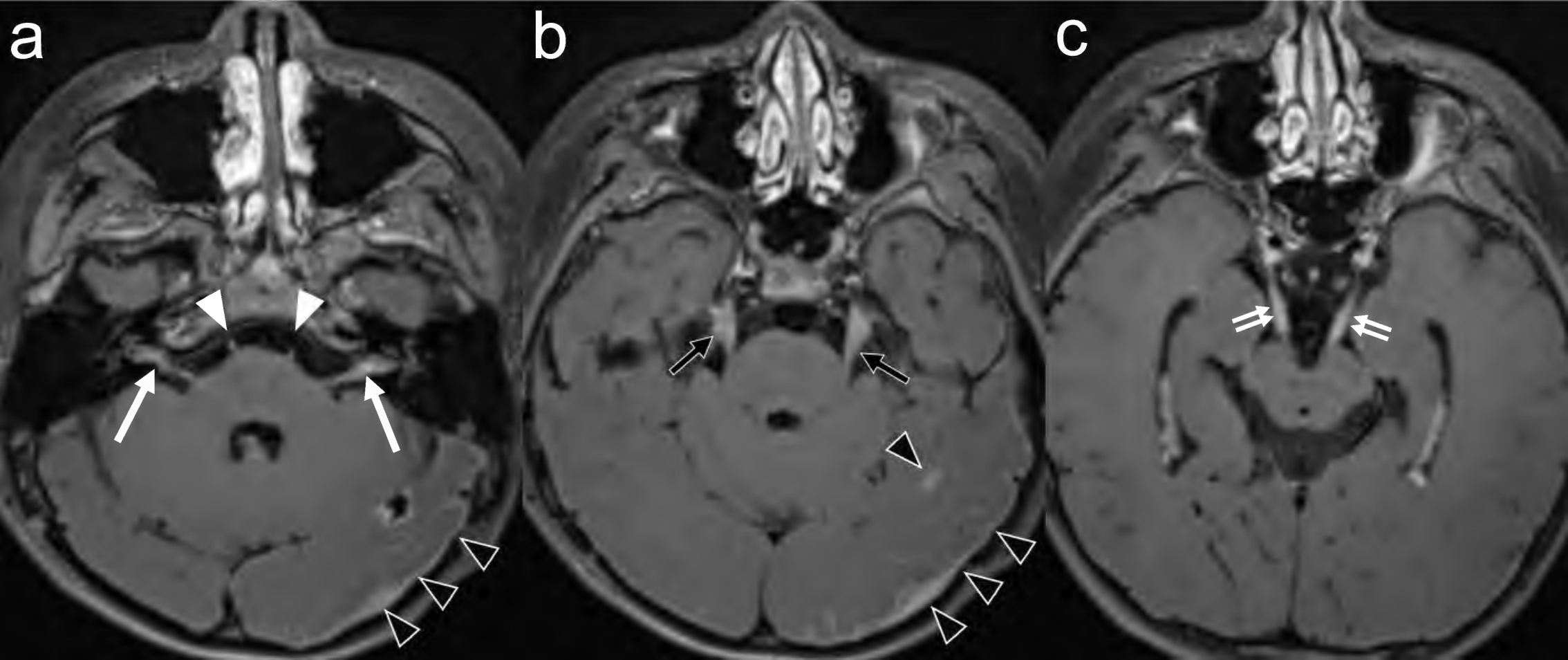
a
b
c